Strain-modulated excitonic gaps in mono- and bi-layer $MoSe_2$*

Jianting Ji(籍建葶), Anmin Zhang(张安民), Tianlong Xia(夏天龙), Po Gao(高坡), Yinghao Jie(揭英昊), Qian Zhang(张倩), and Qingming Zhang(张清明)†

Department of Physics, Beijing Key Laboratory of Opto-Electronic Functional Materials & Micro-nano Devices, Renmin University of China, Beijing 100872, *China*

(Received 16 February 2016; revised manuscript received 20 March 2016; published online 1 June 2016)

Photoluminescence (PL) and Raman spectra under uniaxial strain were measured in mono- and bi-layer $MoSe_2$ to comparatively investigate the evolution of excitonic gaps and Raman phonons with strain. We observed that the strain dependence of excitonic gaps shows a nearly linear behavior in both flakes. One percent of strain increase gives a reduction of ~ 42 meV (~ 35 meV) in A-exciton gap in monolayer (bilayer) $MoSe_2$. The PL width remains little changed in monolayer $MoSe_2$ while it increases rapidly with strain in the bilayer case. We have made detailed discussions on the observed strain-modulated results and compared the difference between monolayer and bilayer cases. The hybridization between 4d orbits of Mo and 4p orbits of Se, which is controlled by the Se–Mo–Se bond angle under strain, can be employed to consistently explain the observations. The study may shed light into exciton physics in few-layer $MoSe_2$ and provides a basis for their applications.

Keywords: photoluminescence, strain, low-dimensional semiconductors

PACS: 78.55.–m, 78.30.–j, 63.22.Np **DOI:** 10.1088/1674-1056/25/7/077802

1. Introduction

Most transition metal disulfides MX_2 (M = Mo, W, Ta, Re; X = S, Se, Te) are semiconductors with outstanding performance and have been widely investigated and applied. Two-dimensional MX_2 has the similar intra-layer honeycomb lattice as graphene and the van der Waals interaction is responsible for the weak interlayer coupling. This allows one to obtain few-layer MX_2 flakes by mechanical exfoliation from bulk crystals just like graphene. Compared to pristine graphene with zero energy gap, MX_2 has a gap of 1–2 eV, which is a large advantage for applications.[1–3] Furthermore, its higher mobility[4] is particularly essential to semiconducting devices such as logical devices,[3,5] sensors,[6] photo-diodes,[7] and photo-detectors.[8] The unique valley polarization revealed in MX_2 provides us with a new degree of freedom for device design.[3,9–13]

External strain is a conventional and convenient way to tune energy gap and lattice vibrations in low-dimensional semiconductors. The subtle changes induced by strain can be easily probed by the micro-Raman technique. In fact, the strain-modulated effects have been extensively investigated in graphene[14,15] and MoS_2.[16–19] First-principles calculations predicted that strain can substantially change the band structure of monolayer MX_2 and drive a transition from direct gap to indirect gap.[20–24] Interestingly, strain can also modulate magnetic properties of few-layer MX_2[20,21] and provide possible scenarios for some optical devices or solar cells.[25] Among few-layer MX_2 compounds, $MoSe_2$ has attracted special attention since its energy gap under zero strain (~ 1.55 eV), is exactly close to the optimum value balanced between the optimum utilization of the solar spectrum and the maximum efficiency of conversion into electricity.[26] This means that two-dimensional $MoSe_2$ may play an important role in the future opto-electric applications.

In this work, we carried out careful Raman scattering studies of strain-induced effects in mono- and bi-layer $MoSe_2$. The linear dependence of energy gaps on strain was observed and quantitatively determined. The strain effect can be well understood in term of the change of Se–Mo–Se bond angle. We have comparatively discussed the strain effects, which may help us get insight into exciton physics in $MoSe_2$ and provide a solid basis for applications.

2. Experimental methods

$MoSe_2$ bulk crystals were grown through vapor transport equilibration under strict conditions.[27] Similar to graphene, mono- and bi-layer $MoSe_2$ flakes used in this work were mechanically exfoliated from bulk crystals but transferred to flexible polyethylene terephthalate (PET) substrate instead of conventional SiO_2/Si substrate, to carry out measurements under strain. As shown in Fig. 1(a), the monolayer piece is a nearly isosceles triangular area with a side length of ~ 8 microns. The bilayer piece is the neighboring parallelogram. Monolayer $MoSe_2$ flake was determined by the A_{1g} phonon frequency

*Project supported by the National Basic Research Program of China (Grant No. 2012CB921701) and the National Natural Science Foundation of China (Grant Nos. 11474357 and 11004245). Qingming Zhang and Tianlong Xia were supported by the Fundamental Research Funds for the Central Universities of China and the Research Funds of Renmin University of China.

†Corresponding author. E-mail: qmzhang@ruc.edu.cn

© 2016 Chinese Physical Society and IOP Publishing Ltd

(240.5 cm^{-1}, Fig. 1(b)) and the PL peak position located at 1.55 eV. The extremely strong PL intensity under very low-intensity excitation light further confirmed its thickness since it is a direct-gap semiconductor only in the monolayer case. Then one can further determine the bilayer flake which becomes an indirect-gap semiconductor and its PL intensity is lower than the monolayer case by a factor of $\sim 1/20$.

The home-made setup for applying strain is illustrated in Fig. 1(c). By changing the screw positions, one can adjust the curvature radius of the PET substrate.[18] External strain can be applied to the flakes through the mediation of van der Waals interaction between flake and substrate. The calculation details can be found in Fig. 1(d). The applied strain e is defined as $e = d/2R$ in units of mm. The maximum applied strain was limited to 0.75%, since the flake may slip off from the substrate under a strain higher than 0.8%.[18]

PL and Raman scattering measurements were performed with a Jobin–Yvon HR800 system equipped with liquid-nitrogen cooled CCD and a He–Ne excitation laser of 633 nm (MellesGriot). The configuration of backscattering was adopted in our measurements. The laser power was monitored and controlled at a level of 60 μW to protect the flakes and the focus spot is around 2 microns in diameter. All the measurements were carried out at room temperature.

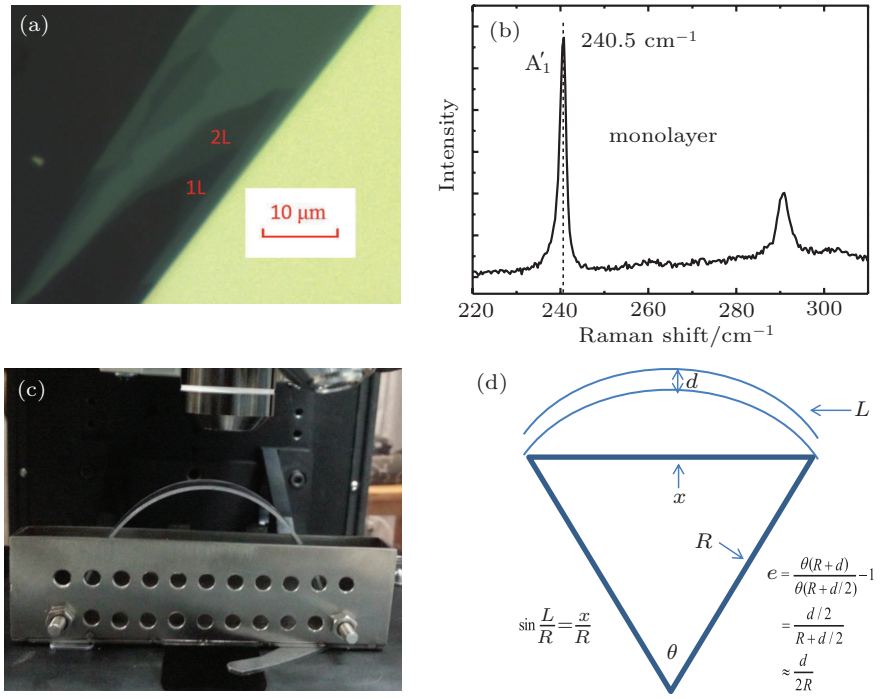


Fig. 1. (color online) (a) Optical image of monolayer and bilayer $MoSe_2$. (b) Raman phonon in the monolayer case. (c) Home-made setup for applying strain on films. (d) Schematic of quantitatively estimated strain. The arc length of bended PET substrate is L and its thickness is d. If the straight-line distance between any two points on the PET substrate is taken as x, one can calculate the radius of curvature R. Tuning R by changing x gives variable strains e. For accuracy, the two points should be as close as possible to the arc top.

3. Results and discussion

PL spectra of mono- and bi-layer $MoSe_2$ under various strains are shown in Fig. 2. The evolutions of PL peaks with strain are distinguished in two flakes. PL peak position or energy gap of A-exciton moves down almost linearly with increasing strain in the monolayer sample, and its width remains little changed. In bilayer $MoSe_2$, PL intensities are significantly weakened because of its indirect gap. Its position has the similar linear strain dependence but its width is obviously reduced by strain. The PL peak positions and widths extracted from Fig. 2 are summarized in Fig. 3. The linear behaviors are clearly seen in both samples in Fig. 3. The fitting in the monolayer case gives a slope of -42 meV/% strain, which is well consistent with first-principles calculations using the GGA method.[28,29] The calculated rate of strain change is -45 meV/% strain for the direct gap. In the bilayer sample, the fitted slope is -35 meV/% strain, slightly smaller than that in the monolayer case. In comparison, the slope is -45 meV/% strain and -53 meV/% strain in mono- and bilayer MoS_2,[17] respectively. Considering the different energy gaps (1.55 eV and 1.82 eV for monolayer $MoSe_2$ and MoS_2, respectively), we obtained the rate of energy-gap change with strain, $\sim 2.7\%$ per 1% strain for $MoSe_2$ and $\sim 2.4\%$ per 1% strain for MoS_2. This means that the excitonic gap of $MoSe_2$ is even more sensitive to strain than MoS_2. However, this is reversed in the bilayer case, i.e., 2.3% per 1% strain for $MoSe_2$ and 2.9% per 1% strain for MoS_2.

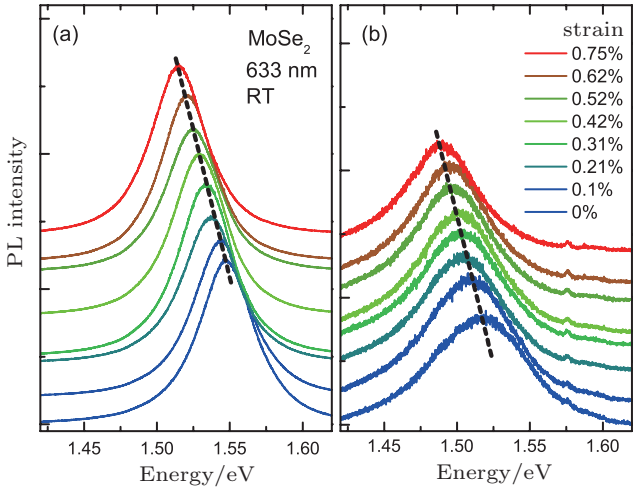


Fig. 2. (color online) PL spectra in monolayer (a) and bilayer (b) $MoSe_2$ with applying strain from 0 to 0.75%.

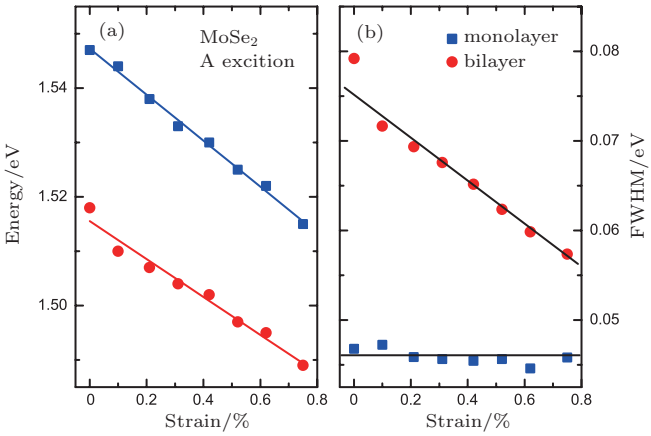


Fig. 3. (color online) (a) Strain dependence of A-exciton PL peak positions in mono- and bi-layer $MoSe_2$. (b) Strain dependence of A-exciton PL peak widths in mono- and bi-layer $MoSe_2$.

The difference can be understood in terms of the different interlayer coupling in both samples. Generally the uniaxial strain stretches the Mo–Se bond and reduces the Se–Mo–Se bond angle. The valence bands of $MoSe_2$ contain five d orbits of Mo and 4p orbits of Se. In detail, the conduction bands at K points and the valence bands at Γ points are dominated by d_{z}^{2} orbits, while $d_{x^2-y^2}$ and d_{xy} orbits contribute to the valence bands at K points. The rest d_{xz}, d_{yz} orbits and 4p orbits of Se have a smaller contribution. The application of in-plane uniaxial strain increases the distance between Mo and Se atoms and reduces the Mo–Se–Mo bond angle. Consequently, it brings an effective increase of the vertical distance between Mo and Se atoms, and hence a reduction of the hybridization between p_z orbits of Se and d_{z}^{2} orbits of Mo. This moves down the bottom of the conduction bands at K points and moves down the top of the valence bands at Γ points.

On the other hand, the decrease of the Mo–Se–Mo bond angle under strain reduces the distance between Mo and Se layers. This enhances the coupling between p_x/p_y orbits of Se and $d_{x^2-y^2}$ and d_{xy} orbits of Mo. However, the absolute distance between Mo and Se is against the enhancement. The net effect of strain on the valence band top becomes very small. Taking all the factors discussed above, we will see that strain modulates the direct gap at K points by changing the conduction band bottom and keeping the valence band top fixed. Larger strain gives a smaller gap and vice versa. If strain is too large to move up the valence band top at Γ points over that at K points, monolayer $MoSe_2$ will become an indirect-gap semiconductor.[20–24,28–30]

Figure 3(b) shows the evolution of PL peak width with strain. Under zero strain, the PL peak of the bilayer sample is about two times wider than that in the monolayer one. The width remains unchanged with strain in monolayer $MoSe_2$, while it clearly becomes sharper with strain in the bilayer sample. This can also be explained by the reduction of Se–Mo–Se bond angle under strain.[30] The angle reduction effectively decreases the thickness of the $MoSe_2$ layer or is equivalent to the increase of the interlayer distance, which weakens the interlayer coupling and decreases the A-exciton PL peak width.

4. Summary

We first observed the direct energy-gap evolution with strain in mono- and bilayer $MoSe_2$. The measured rates of change are consistent with the calculated ones. We further discussed the possible mechanisms in both cases in terms of interlayer coupling. The reduction of the Mo–Se–Mo bond angle under strain modifies the hybridization between the d orbits and p orbits of Se, and further shifts the conduction and valence bands. This effectively reduces the band gap. The studies on excitonic energy gaps under strain are important to the applications and provide fundamental insight to exciton physics in this two-dimensional system.

References

[1] Mak K F, Lee C, Hone J, Shan J and Heinz T F 2010 *Phys. Rev. Lett.* **105** 136805
[2] Splendiani A, Sun L, Zhang Y, Li T, Kim J, Chim C Y, Galli G and Wang F 2010 *Nano Lett.* **10** 1271
[3] Xiao D, Liu G B, Feng W, Xu X and Yao W 2012 *Phys. Rev. Lett.* **108** 196802
[4] Radisavljevic B, Radenovic A, Brivio J, Giacometti V and Kis A 2011 *Nat. Nanotechnol.* **6** 147
[5] Radisavljevic B and Kis A 2013 *Nat. Mater.* **12** 815
[6] Perkins F K, Friedman A L, Cobas E, Campbell P M, Jernigan G G and Jonker B T 2013 *Nano Lett.* **13** 668
[7] Sundaram R S, Engel M, Lombardo A, Krupke R, Ferrari A C, Avouris P and Steiner M 2013 *Nano Lett.* **13** 1416
[8] Yin Z, Li H, Li H, Jiang L, Shi Y, Sun Y, Lu G, Zhang Q, Chen X and Zhang H 2012 *ACS Nano* **6** 74
[9] Xiao D, Yao W and Niu Q 2007 *Phys. Rev. Lett.* **99** 236809
[10] Yao W, Xiao D and Niu Q 2008 *Phys. Rev. B* **77** 235406
[11] Cao T, Wang G, Han W, Ye H, Zhu C, Shi J, Niu Q, Tan P, Wang E, Liu B and Feng J 2012 *Nat. Commun.* **3** 887
[12] Mak K F, He K, Shan J and Heinz T F 2012 *Nat. Nanotechnol.* **7** 494

[13] Zeng H, Dai J, Yao W, Xiao D and Cui X 2012 *Nat. Nanotechnol.* **7** 490
[14] Huang M, Yan H, Chen C, Song D, Heinz T F and Hone J 2009 *Proc. Natl. Acad. Sci. U.S.A.* **106** 7304
[15] Mohiuddin T M G, Lombardo A, Nair R R, Bonetti A, Savini G, Jalil R, Bonini N, Basko D M, Galiotis C, Marzari N, Novoselov K S, Geim A K and Ferrari A C 2009 *Phys. Rev. B* **79** 205433
[16] Rice C, Young R J, Zan R, Bangert U, Wolverson D, Georgiou T, Jalil R and Novoselov K S 2013 *Phys. Rev. B* **87** 081307(R)
[17] Conley H J, Wang B, Ziegler J I, Haglund R F, Jr., Pantelides S T and Bolotin K I 2013 *Nano Lett.* **13** 3626
[18] Zhu C R, Wang G, Liu B L, Marie X, Qiao X F, Zhang X, Wu X X, Fan H, Tan P H, Amand T and Urbaszek B 2013 *Phys. Rev. B* **88** 121301(R)
[19] He K, Poole C, Mak K F and Shan J 2013 *Nano Lett.* **13** 2931
[20] Lu P, Wu X, Guo W and Zeng X C 2012 *Phys. Chem. Chem. Phys.* **14** 13035
[21] Pan H and Zhang Y W 2012 *J. Phys. Chem. C* **116** 11752
[22] Li T 2012 *Phys. Rev. B* **85** 235407
[23] Shi H, Pan H, Zhang Y W and Yakobson B I 2013 *Phys. Rev. B* **87** 155304
[24] Horzum S, Sahin H, Cahangirov S, Cudazzo P, Rubio A, Serin T and Peeters F M 2013 *Phys. Rev. B* **87** 125415
[25] Feng J, Qian X, Huang C W and Li J 2012 *Nat. Photo.* **6** 865
[26] Loferski J J 1956 *J. Appl. Phys.* **27** 777
[27] Bougouma M, Batan A, Guel B, Segato T, Legma J B, Reniers F, Delplancke-Ogletree M P, Buess-Herman C and Doneux T 2013 *J. Cryst. Growth* **363** 122
[28] Kumar A and Ahluwalia P K 2013 *Physica B-Conden. Matt.* **419** 66
[29] Kumar A and Ahluwalia P K 2013 *Modelling Simul. Mater. Sci. Eng.* **21** 065015
[30] Chang C H, Fan X, Lin S H and Kuo J L 2013 *Phys. Rev. B* **88** 195420